# Recent Studies in Fast Electron Energy Transport Relevant to Fast Ignition Inertial Fusion

P.A. Norreys 1)2), R.H.H. Scott 1),2) K.L. Lancaster 1), J.S. Green 1),2), A.P.L. Robinson 1), M. Sherlock 1), R.G. Evans 2), M. G. Haines 2), S. Kar 3), M. Zepf 3), M.H. Key 4), J. King 5), T. Ma 5), T. Yabuuchi 5), M.S. Wei 5), F.N. Beg 5), P. Nilson 6), R.B. Stephens 7), J. Valente 8), J.R. Davies 8) K. Takeda 9), H. Azechi 9), M. Nakatsutsumi 10), T. Tanimoto 10), R. Kodama 9),10) and K.A. Tanaka 10).

1) STFC Rutherford Appleton Laboratory, Harwell Science and Innovation Campus, Didcot, Oxfordshire OX11 0QX, United Kingdom
2) Imperial College London, Prince Consort Road, London SW7 2BZ, United Kingdom
3) Queens University Belfast, University Road, Belfast BT7 1NN, United Kingdom.
4) Lawrence Livermore National Laboratory, Livermore CA, USA
5) Department of Mechanical and Aerospace Engineering, University of California San Diego, 9500 Gilman Drive 0411, La Jolla, California 92093-0411, USA
6) Laboratory for Laser Energetics, University of Rochester, 250 East River Road, Rochester, NY, USA.
7) General Atomics Corp., San Diego, USA.
8) Grupo de Lasers e Plasmas, Insituto de Plasmas e Fusão Nuclear Instituto Superior Técnico, Av. Rovisco Pais, 1049-001 Lisbon, Portugal.
9) Institute of Laser Engineering, Osaka University, Japan.
10) Graduate School of Engineering, Osaka University, Japan.

**Abstract.** The first results of an experimental campaign are reported in which it is intended to demonstrate whether it is possible for the fast electron beam (produced at irradiances in excess of $10^{19}$ $Wcm^{-2}\mu m^2$) to be artificially collimated even when the beam enters the target with a large divergence angle. The artificial collimation occurs because of a pre-generated magnetic field that is produced by a laser pulse of $10^{18}$ $Wcm^{-2}\mu m^2$ that precedes the main pulse. The first experiment to examine the double pulse collimation concept has revealed evidence for single-pass heating for Ti foils of ≤ 25 μm thickness irradiated by the double pulse. This may be evidence for magnetic field generation in the dense plasma that prevents refluxing of the fast electrons from the rear surface. There was no evidence for collimation of the main pulse for these conditions. The most likely explanation for the lack of collimation is the generation of competing hollowing and focusing magnetic fields that arise as a result of the hydrodynamic shock induced by the low intensity pedestal of the laser pulse. The implications of these results are discussed and future directions outlined. In addition, a new analytic model is presented that reproduces the intensity scaling results of Beg et al. [F.N.Beg et al., Phys. Plasmas **4**, 447 (1997)] and the new data at intensities up to $10^{21}$ $Wcm^{-2}$.

## 1. Introduction

The first results of an experimental campaign are reported in which it was intended to demonstrate whether it is possible for the fast electron beam (produced at irradiances in excess of $10^{19}$ $Wcm^{-2}\mu m^2$) to be artificially collimated even when the beam enters the target with a large divergence angle. The artificial collimation occurs because of a pre-generated magnetic field that is produced by a laser pulse of $10^{18}$ $Wcm^{-2}\mu m^2$ that precedes the main pulse.

Atzeni [1] showed that for ignition of preformed DT plasma with compressed core density of 400 $gcm^{-3}$, at least 11 kJ must be deposited in the hot-spot region with a radius of up to 15 μm (0.6 g $cm^{-2}$) and a length of up to 30 μm (1.2 g $cm^{-2}$) in a time less than the inertial confinement time (16 ps). The electron energy required to give a stopping distance of 1.2 g $cm^{-2}$ in 400 g $cm^{-3}$ DT is 1.4 MeV (that varies weakly with density). Matching this energy to the ponderomotive potential gives an $I\lambda^2$ of $1.5\times 10^{19}$ W $cm^{-2}$ $\mu m^2$. This is lower than the

values that can achieved by the current generation of high-intensity lasers such as Vulcan PW, but on the other hand these machines provide pulse durations much smaller than that required by fast ignition (≤ 1 ps).

For these reasons, we carried out an experimental campaign on the Vulcan PW laser using pulse durations of 5 - 10 ps, giving values of both $I\lambda^2$ and pulse duration comparable to those that would be required for an ignition laser, which are two key parameters in determining the physics of laser-plasma interactions. The spot radius and pulse energy were, however, much lower than those required for an ignition laser. Obtaining all of the required laser parameters simultaneously is clearly only possible with a laser far larger than any that currently exists.

We measured the divergence of the electrons accelerated into the target, which is a crucial parameter in determining the coupling of the electrons to the hotspot in fast ignition [2]. The divergence was found to be 29° (±7°) and 32° (±18°) by X-ray $K_\alpha$ imaging and optical shadowgraphy, respectively at $1.5\times10^{19}$ $Wcm^{-2}$ and 35° (±13°) at $4\times10^{19}$ $Wcm^{-2}$. An intensity dependence to the beam divergence has been revealed for the first time when these divergence measurements were compared with other measurements reported in the literature (see Figure 1).

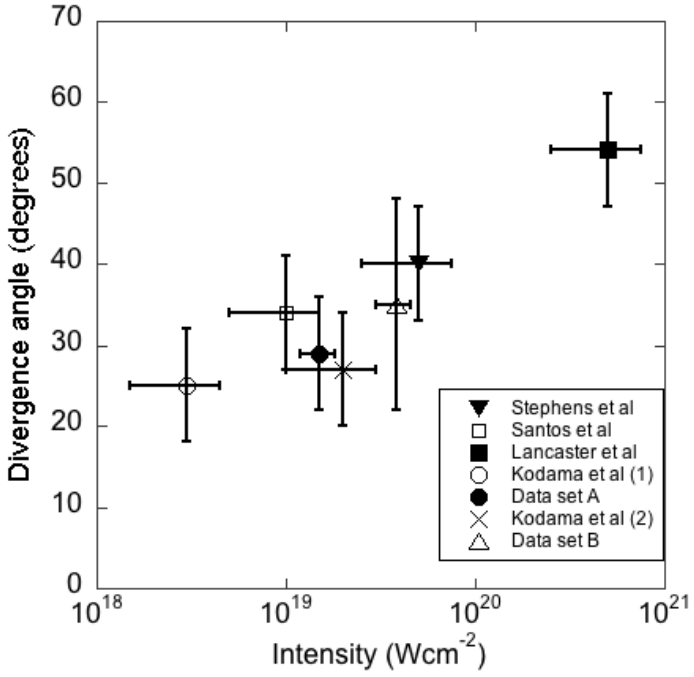


*Figure 1. Divergence angle as a function of intensity on target. From reference [3].*

Both the experiment and theory indicate that for realistic fast ignition beam energies (i.e. ≤ 100 kJ), the irradiance on target is limited to $I\lambda^2$ of $5\times 10^{19}$ W $cm^{-2}$ $\mu m^2$, unless further measures are taken to control the beam divergence pattern. The HiPER beam operating at $2\omega_0$ delivering 70 kJ in 16 ps to a focal spot of 40 μm gives an irradiance on target of $9\times10^{19}$ $Wcm^{-2}$ $\mu m^{-2}$. Control of the fast beam divergence appears to be necessary to the success of the project. This is also important to other areas of research relevant to the HiPER such as X-ray back-lighters and high-temperature material properties.

Two-dimensional (2D) particle-in-cell (PIC) simulations using the OSIRIS framework confirmed that the divergence effect is independent of focal spot radius. The divergence is

primarily governed by the small scale break up of the critical surface due to a Rayleigh Taylor-like rippling instability but is clearly affected by the laser wavelength as well. These results have recently been published in reference [3].

The leading approach to control the beam divergence pattern is the vacuum gap method proposed by Campbell et al. [4] The idea has a great deal of merit as collimation and guiding of MeV electrons has been observed in cone-wire plasmas [5], although at distances > 200 μm from the cone-tip, we have shown that the energy is transported close to the wire surface, by comparison of interferometric measurements of the expansion of the wire with hydrodynamic and hybrid particle-in-cell simulations [6]. This approach demands additional target engineering of the cone, and one must ensure that the vacuum gaps in the cone itself are not filled by plasma.

As detailed below, the experiment revealed evidence for single-pass heating for Ti foils of ≤ 25 μm thickness irradiated by the double pulse. This is likely to result from magnetic field generation in the dense plasma that prevents refluxing of the fast electrons from the rear surface. There was no evidence for collimation of the main pulse for these conditions. The most likely explanation for the lack of collimation is the generation of competing hollowing and focusing magnetic fields that arise as a result of the hydrodynamic shock induced by the low intensity pedestal of the laser pulse.

## 2. Modelling

A new approach has been proposed that does not suffer from these problems (see reference [7] for further details). We have used the recently developed the LEDA code to numerically demonstrate artificially induced collimation in 2D Cartesian geometry. LEDA is a novel 2D hybrid-Vlasov-Fokker-Planck code that treats the fast electrons via an algorithm similar to the KALOS code of Bell and Kingham [8], whilst the background plasma is treated in the fashion of Davies' hybrid code [9].

The effect can be seen by comparing two simulations with solid Al targets. In run 'A' there are two 500 fs pulses of fast electrons, the first corresponding to $2.5\times10^{18}$ $Wcm^{-2}$ irradiation ($T_f$ ~200 keV, 24° half-angle), and the second corresponding to $5\times10^{19}$ $Wcm^{-2}$ irradiation ($T_f \sim 2$ MeV, 47° half-angle). In both cases a 5 $\mu$m Gaussian injection spot was used. In run 'B' there is only the high intensity pulse.

In Figure 2 we compare 'A' and 'B' at 900 fs and 400 fs respectively. At these times there have been 400 fs of the high intensity pulse in both cases. Figure 2 clearly shows that when the low intensity pulse precedes the high intensity pulse the fast electrons are all collimated into a tight beam of 20 $\mu$m width. Without the low intensity pulse the fast electrons are not collimated, and are a divergent spray.

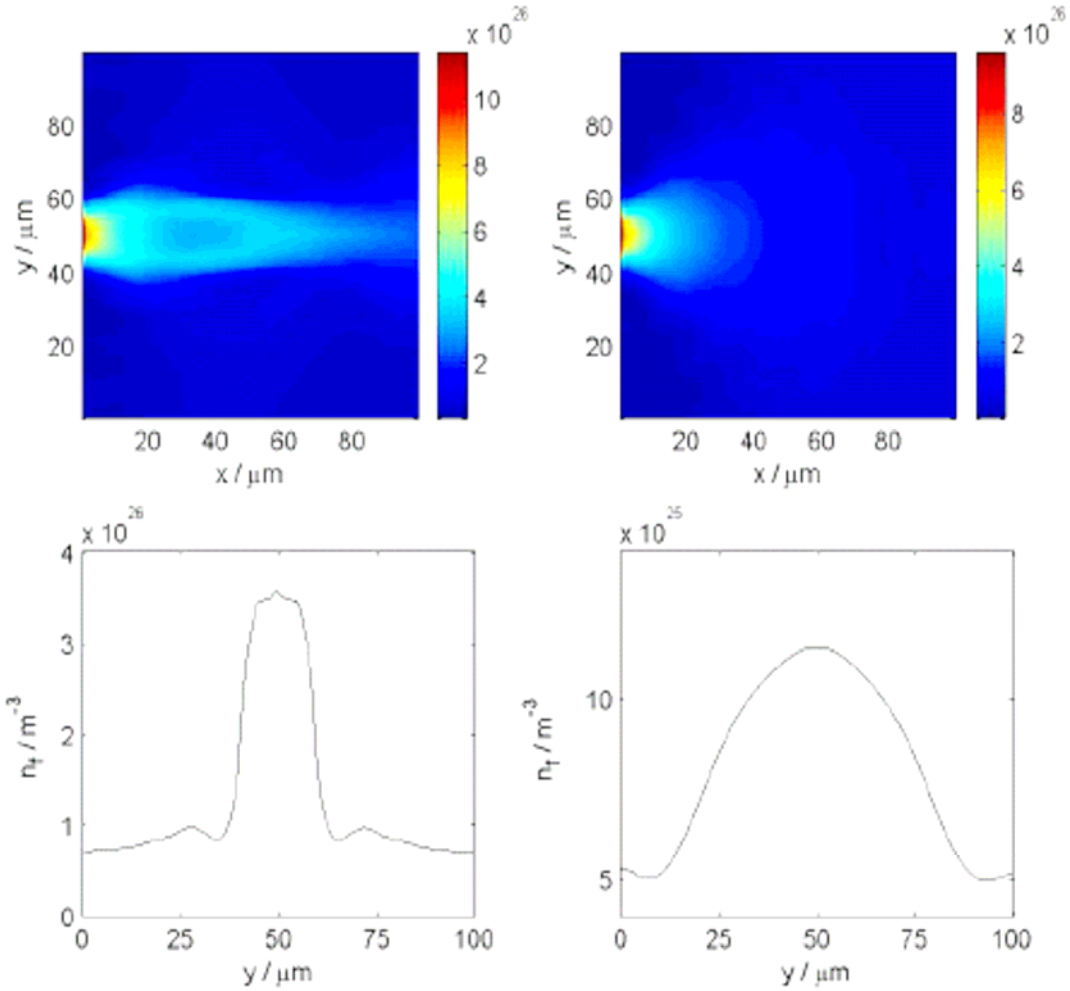


*Figure 2. Fast electron density at 900 fs in run 'A' (top left) and 400 fs in run 'B'. Bottom figures are lineouts at x = 50 µm*

A full suite of well-tested plasma diagnostics were used for this investigation. These included Cu $K_\alpha$ imaging; time-resolved optical imaging of the thermal radiation from the rear surface, transverse optical probe; X-ray pinhole imaging; X-ray spectrometers (HOPG and conically curved KAP) and a single hit charge coupled device (CCD) spectrometer.

## 3. Double pulse experiment

Tiitanium targets were shot at normal incidence and were varied in thicknesses from 10 µm to 140 µm. Table 1 summarises the parameter space investigated during the experiment.

| Energy (J) | Pulse Length (ps) | Pulse Separation (ps) | Pulse 1 Intensity ($W/cm^2$) | Pulse 2 Intensity ($W/cm^2$) |
|---|---|---|---|---|
| 300 | 5 | X | X | 5E19 |
| " | " | 7.5 | 2E18 | 5E19 |
| " | " | 15 | " | " |
| 50 | 0.5 | X | X | 8E19 |
| " | " | 1.5 | 3E18 | 8E19 |

*Table 1: Shot energy, pulse length, pulse separation and the intensities of the two pulses. The X's denote where only a single pulse was used for reference.*

In this paper, we will concentrate on unexpected features observed using rear surface temperature diagnostic HISAC [10]. The temporal evolution of the rear surface thermal radiation was imaged in 2D in the spectral region between $\omega_0$ to $2\omega_0$. $2\omega_0$ coherent transition radiation was removed by the use of dichoric filters. Optical fibres were used to convert the 2D thermal image of the target rear surface into a 1D image which was then streaked in time. The resulting image was 4 dimensional (2 space, 1 time and 1 intensity). By deconvolving this image and assuming a Planckian radiation spectrum, the 2D temporal evolution of the rear surface temperature was obtained. Absolute calibration of the device using the X-ray diagnostics has yet to be performed for this experiment – that analysis is still underway. A preliminary estimate of rear surface temperatures has been made by comparing the results with those obtained from previous experiments performed on the same facility in a similar parameter regime [10].

**4. Results**

The results for the two pulse duration (0.5 ps and 5 ps) regimes investigated are summarised in figures 3 and 4. Both show similar characteristic features; single pulse interactions used for normalisation purposes show a double temperature gradient for both pulse durations used, as observed in previous experiments [10]. On the other hand, the double pulse results for both pulse durations have significantly reduced rear surface temperature for thin targets (areal electron density ~ $10^{25}$ $m^{-2}$) and in both cases the double gradient is not present.

In the event that collimation had occurred a clear increase in rear surface temperature would have been expected for the double pulse results, particularly for the thicker targets (whose electron areal density > $5\times10^{25}$ electrons $m^{-2}$). As this increase was not observed, it confirms that beam collimation did not occur. This result is further supported by the 2D $K_\alpha$ data (shown in figure 5); there is no clear reduction in the $K_\alpha$ spot size with the introduction of the double laser pulse, as would be expected if collimation was occurring.

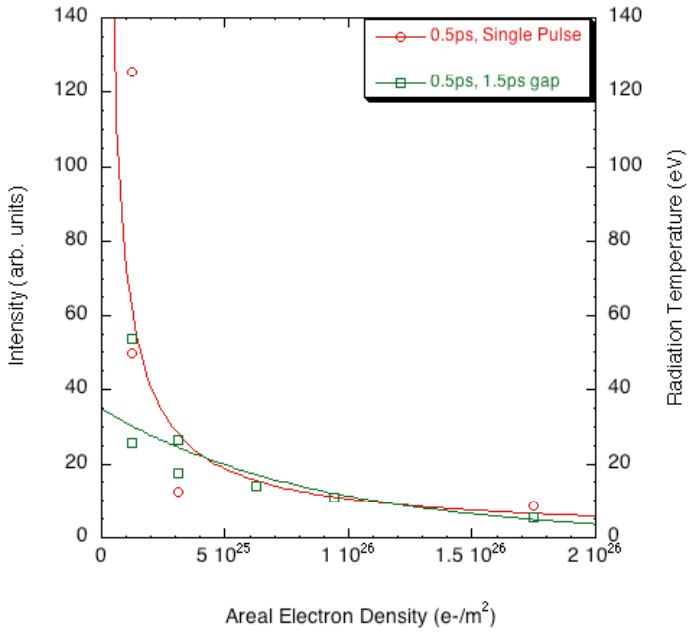


*Figure 3. 50 J, 0.5 ps pulse length, rear surface optical emission results. Variation in peak rear surface radiation intensity and estimated radiation temperature with areal electron density.*

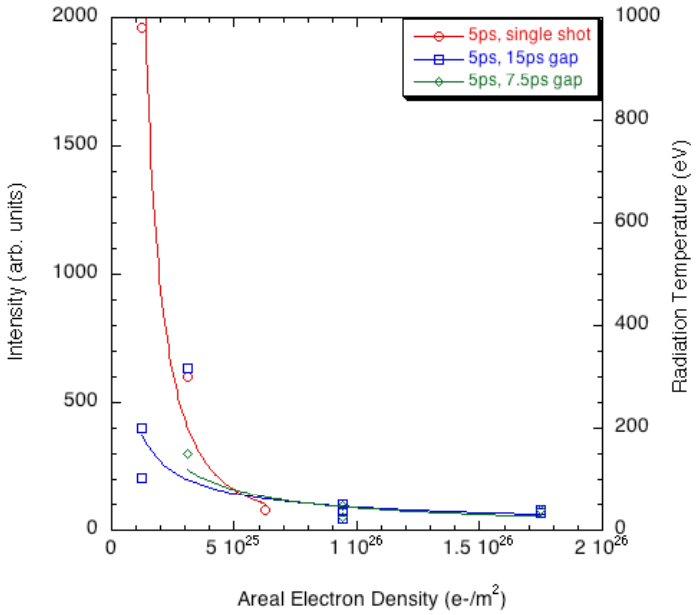


*Figure 4. 300 J, 5 ps pulse length rear surface optical emission results. Variation in peak rear surface radiation intensity and estimated radiation temperature with areal electron density.*

## 5. Discussion

The lack of a double gradient in simulations of previous experiments [10] was explained by the generation of an azimuthal magnetic field inside the solid density plasma that prevented refluxing fast electrons from the rear surface returning to the focal region. This resulted in a

reduced temperature and was attributed to single pass heating that resulted from the electron motion in the magnetised plasma. The same observation in this experiment might be thought to be at odds with the apparent lack of collimation. This is not necessarily true. The lack of collimation implies that the azimuthal magnetic field is insufficient to collimate the beam, but it does not imply that there is no magnetic field there at all.

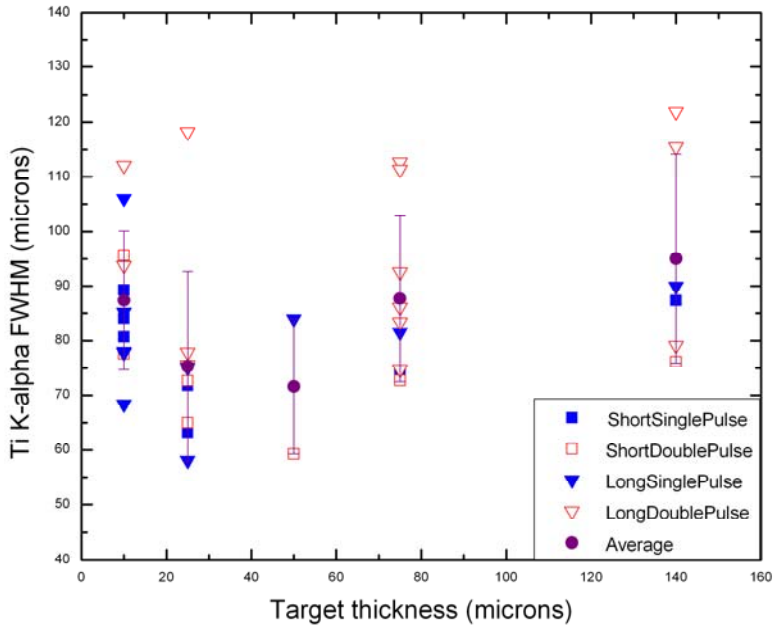


*Figure 5. 2D Ti $K_\alpha$ results. Variation in FWHM spot size with target thickness. No clear reduction in spot size was observed with the introduction of the double laser pulse.*

The failure to realise two-pulse collimation in this experiment clearly needs to be fully explained. The LEDA code has been used post-experiment to numerically investigate effects of density perturbations and artificially induced collimation in 2D Cartesian geometry. The effect of the hydrodynamic shock can be seen by comparing the B-field and fast electron density in the generator pulse corresponding to $2.5\times10^{18}$ Wcm$^{-2}$ irradiation ($T_f$ ~200 keV, 24° half-angle). A 5 $\mu$m diameter Gaussian injection spot was used. Two simulations were performed. In the first, a linear density ramp from $n_c$ (at 0 μm) to solid density (at 10 μm) was compared with the case where an infinite, planar shocked density spike (×1.5 solid density) was introduced at 10 μm. The results of the B-field and fast electron density are shown in Figures 6 and 7 for the latter case.

One can see that a reversed, hollowing field has developed from 10 μm to 30 μm in Figure 6. The result is that, instead of a collimated flow of fast electrons as one might expect for these low intensity conditions (i.e. similar to those shown in Figure 2), the fast electrons are more divergent (Figure 7). We believe that this is the most plausible cause of the lack of collimation observed in the experiment. It also points to the solution: to reduce or eliminate the spatial extent of the shock compressed region. That way, one recovers the collimated transport pattern shown in Figure 2 and reported in reference [7]. The reduction in size of the pre-formed plasma has other advantages: one can investigate the removal of the barrier to fast electrons entering the target (the bottled up effect [11][21]). The model may have to be refined further to include other effects.

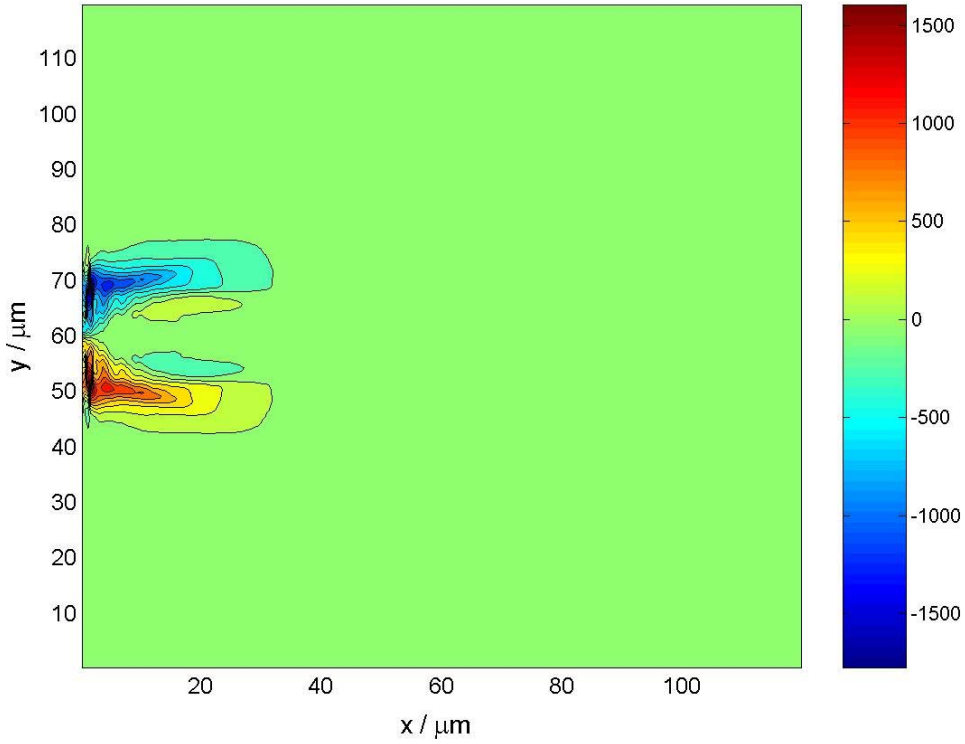


*Figure 6. Spatial profile of the magnetic field (in Tesla) induced after 500 fs. The laser is incident from the left. The reversed magnetic field inside the dense plasma after the shock front is evident from 10 μm – 30 μm.*

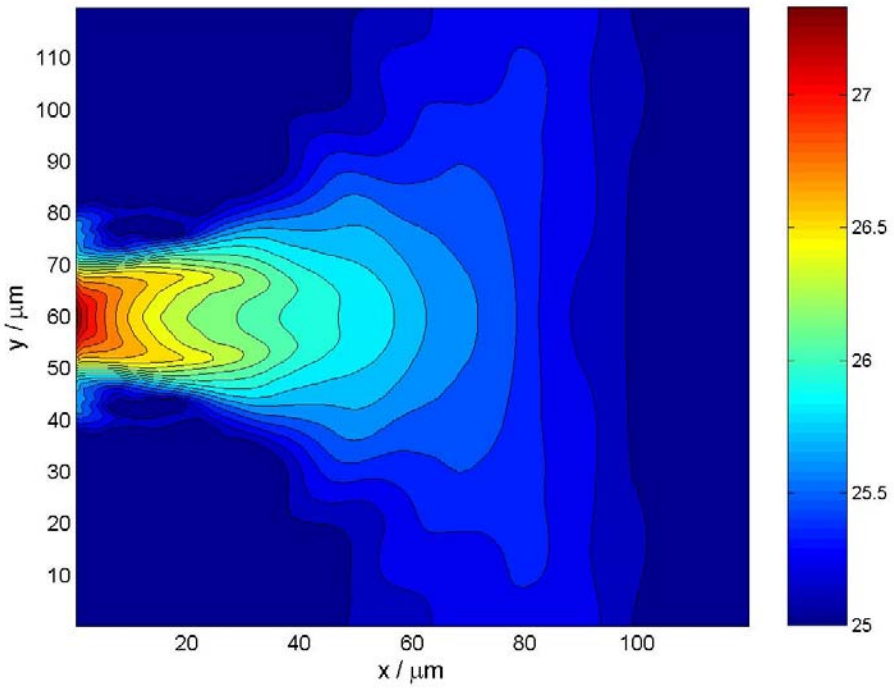


*Figure 7. Spatial profile of the fast electron density after 500 fs.*

## 6. Scaling of the hot electron temperature with intensity on target

Experiments [12] in which the laser pulse is incident on a planer solid target indicate that the hot electron temperature $T_h$ is given by

$$T_h\,(keV) = 215\left(I_{18}\lambda_{\mu m}^2\right)^{1/3} \qquad (1)$$

for a 1μm laser wavelength with intensity $I_{18}$ (in units of $10^{18}$ $Wcm^{-2}$) in the range 0.03 to 6 giving a hot electron temperature of 70 to 400 keV. These results were derived from x-ray bremsstrahlung measurements and fast electron driven ion acceleration from the target front surface. It might appear from the scaling that this is resonance absorption, but the factor in front is about 3.5 times higher than that for resonance absorption. Furthermore with high contrast laser pulses, it may be possible to minimize pre-plasma production associated with laser pre-pulse, in this case the laser will be incident on an overdense plasma for which resonance absorption does not apply. There is evidence from more recent experiments (see Figure 8 and references [13][14]) that suggests that the one third scaling may extend to higher intensity ( $>10^{20}$ $Wcm^{-2}$), which is a much weaker scaling than the ponderomotive scaling found in PIC (particle-in-cell) simulations [15].

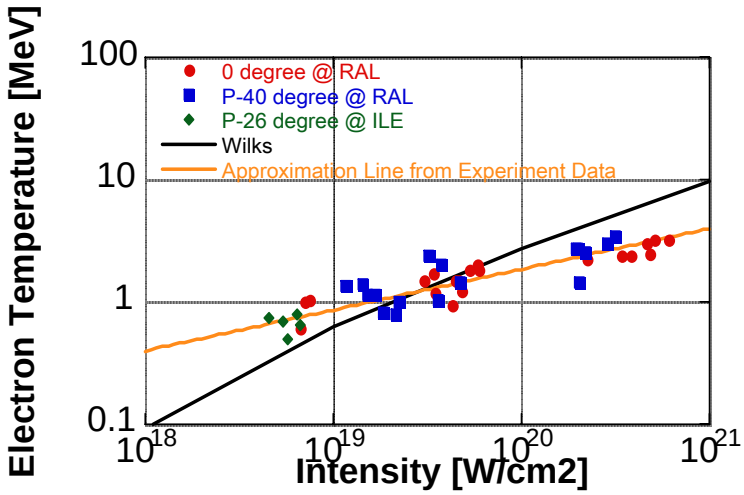


*Figure 8. Hot electron temperature in MeV of the form $dN = E^2exp(-E/kT)dE$ fitted to electron spectra measured at the chamber wall as a function of intensity on target. The laser pulse was both at normal incidence and p-polarised. Results from both the Vulcan and Gekko XII PW laser facilities are included [24].*

One could fit a least squares fit to the experimental points in Figure 8 (this provides the $I^{1/3}$ fit in agreement with references [12 -14]) but this might be misleading for two reasons. Firstly, the electron temperature can be higher than the ponderomotive potential energy when channelling occurs in the coronal plasma [16]. Secondly, the maximum ion energy, which is related to the hot electron temperature in the isothermal expansion model [17], has been shown to scale with $(I\lambda^2)^{0.5}$ above $10^{19}$ $Wcm^{-2}\mu m^2$ for a variety of the irradiation conditions [18][19]. Since the maximum ion energy and electron temperature are related to each other, it would be

inconsistent if their scaling with intensity were different. What is clear from Figure 8 is that Hui Chen's observation of a departure from ponderomotive scaling [13] is robust and occurs under a wide range of irradiation conditions.

While the absorption may lead to average electron energies below the ponderomotive potential energy [20], one would expect some particles at ponderomotive energies. Figure 8 indicates that most of the high energy particles have an energy lower than the ponderomotive potential energy. This suggests that somewhere in between the absorption region and the spectrometer, the fast electrons' energy is being reduced. This could either be due to the formation of the sheath or in part due to the formation of a transport barrier, as seen in simulations presented in reference [21].

A novel explanation for the $I^{1/3}$ intensity scaling recently observed [14] is provided by a theoretical model that has been developed which treats the laser-plasma interaction region as a one-dimensional 'black box' the thickness of which is a few collisionless skin-depths. Conservation equations are applied to this, rather in the same way as in a shock transition. A very simple model has been developed which has the merit in that it reproduces the one-third scaling law for the hot electron temperature in eq.(1), including the proportionality factor. $T_h(keV) = 230\left(I_{18}\lambda^2_{\mu m}\right)^{1/3}$ A fully relativistic model, which, while giving a more complex result, nevertheless agrees to a good approximation reproduces these results. Here $T_h = (1+2^{1/2}a_0)^{1/2} - 1$ A third model includes the effect of reflected light, which deposits twice the relevant photon momentum in the electrons, and makes the electron flux more beam-like; it also shows that laser absorption will reach 80 to 90% at high intensity. These models will be discussed in detail in a forthcoming publication [22].

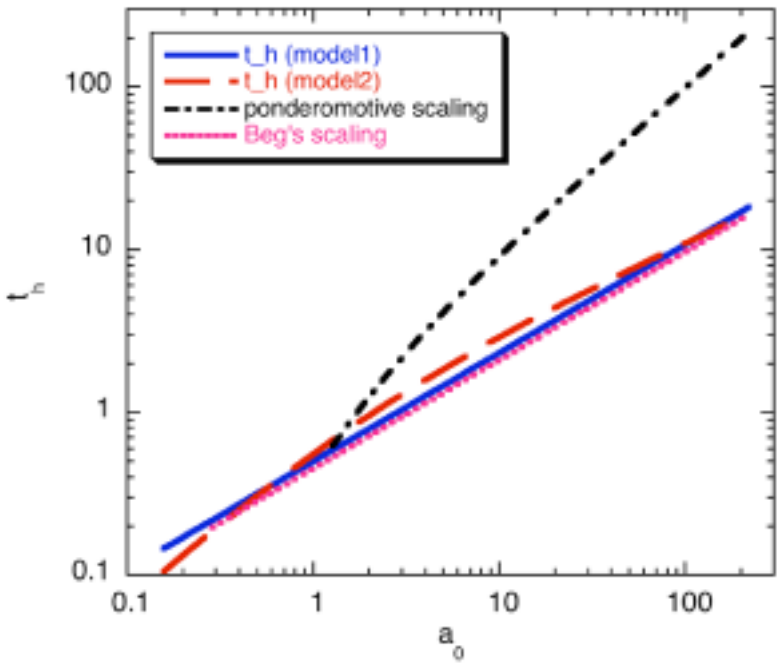


*Figure 9. Plots of Model 1 (Haines classical); Model 2 (Haines relativistic); ponderomotive [23]; and Beg's experimental scaling [12] (eq. (1)) showing the hot electron temperature (normalized to $m_ec^2$) versus $a_0$.*

## 7. Summary

The first experiment to examine the double pulse collimation concept has revealed evidence for single-pass heating for Ti foils of ≤ 25 μm thickness irradiated by the double pulse. This may be evidence for magnetic field generation in the dense plasma that prevents refluxing of the fast electrons from the rear surface. There was no evidence for collimation of the main pulse for these conditions. The most likely explanation for the lack of collimation is the generation of competing hollowing and focusing magnetic fields that arise as a result of the hydrodynamic shock induced by the low intensity pedestal of the laser pulse. New measurements of the electron spectra obtained in an electron spectrometer located on the chamber wall confirm that Chen's observation of a departure from ponderomotive energy [13] is robust and occurs under a range of irradiation conditions. A new theoretical model has been developed that provides an explanation for the $I^{1/3}$ intensity scaling of Beg et al. [12] and new experimental data up to $10^{21}$ $Wcm^2$.

## 8. Acknowledgements

The authors gratefully acknowledge the assistance of the staff of the Central Laser Facility in the planning and delivery of this work. This work was supported by the United Kingdom Science and Technology Facilities Council and the Engineering and Physical Sciences Research Council. American colleagues acknowledge support from the US Department of Energy contract number W-74505-Eng-48. Japanese colleagues gratefully acknowledge support from the Japan Society for the Promotion of Science. MZ acknowledges support from the Royal Society.

## 9. References

1. S.Atzeni, Phys. Plasmas **6**, 3316 (1999).
2. J.Honrubia and J.Meyer-ter-Vehn, Nucl. Fusion **46** L55 (2006).
3. J.S. Green et al., Phys. Rev. Lett. **100**, 015003 (2008).
4. R.B.Campbell et al., Phys. Plasmas **10**, 4169 (2003).
5. R.Kodama et al., Nature (London) **432** (7020) 1005 (2004).
6. J.S. Green et al., Nature Physics **3**, 853 (2007).
7. A.P.L.Robinson et al., Phys. Rev. Lett. **100,** 025002 (2008).
8. A.R.Bell and R.J.Kingham, Phys. Rev. Lett. **91**, 035003 (2003).
9. J.R.Davies, Phys.Rev.E, **65**, 026407, (2002).
10. M. Nakatsutsumi et al, New J. Phys**, 10,** 043046 , (2008).
11. R.G.Evans et al., Appl. Phys. Lett. **86¸** 191505 (2005).
12. F.N.Beg et al., Phys. Plasmas **49**, 447 (1997).
13. H.Chen et al., Bull. Am. Phys. Soc. **50**, 1213 (2005).
14. C.D.. Chen et al., private communication (2008).
15. S.C.Wilks et al., Phys. Rev. Lett. **9**, 1383 (1992).
16. A.Pukhov et al., Phys. Plasmas **6**, 2847 (1999).
17. P.Mora, Phys. Rev. Lett. **90**, 185002 (2003).
18. E.L.Clark et al., Phys. Rev. Lett. **85**, 1654 (2000).
19. L. Robson et al., Nature Phys. **3**, 58 (2007).
20. B. Chrisman et al., Phys. Plasmas 15, 056309 (2008).

21. M.S.Wei et al., Phys. Plasmas **15**, 083101 (2008).
22. M.G. Haines, M. S. Wei, F. N. Beg and R. B. Stephens (submitted to Phys. Rev. Lett.).
23. H. Kho, D. J. Bond, and M. G. Haines, Phys. Rev.A **28**, 3156 (1983).
24. T. Tanimoto et al. (to be published).